Proceedings of the 12th International Conference of Control Systems, and Robotics (CDSR 2025)
July 13, 2025 - July 15, 2025 | Imperial College London Conference Center, London, United Kingdom
Paper No. 123
DOI: 10.11159/cdsr25.123

Model Transfer and Selection Control under Varying and Faulty Conditions

Yunbo Li[1], Long Zhang[2]
[1]The University of Manchester
Oxford Road, Manchester, M13 9PL, UK
yunbo.li@postgrad.manchester.ac.uk; longzhang@manchester.ac.uk

Abstract - Robust and safe control under varying and faulty conditions is paramount for reliable and safe operation of autonomous systems. This paper presents a framework for model transfer and selection control applicable across various autonomous systems of the same type, with one specific case study focusing on unmanned aerial vehicles (UAVs) under varying and faulty conditions. The proposed approach integrates multiple sharing and selection models based control algorithms, enabling the transfer of controllers between different systems of the same type. The effectiveness is validated through real-world experiments and extensive results highlight the potential of model transfer and sharing control methodologies to enhance performance of autonomous system under different operating and faulty conditions.

***Keywords*:** Model transfer, Control, Unmanned Aerial Vehicles,Varying and faulty conditions

1. Introduction

Closed-loop control is unique due to its reliance on negative feedback, which enables tolerance to various uncertainties, including system changes and disturbances. In essence, a single controller in a closed-loop system can perform effectively even when the system undergoes changes or encounters disturbances. However, its performance may degrade under significant system changes, such as those caused by faults, where parameters may shift unexpectedly or hardware components degrade. To address these challenges, adaptive control strategies have been developed to enhance robustness under varying conditions [1-3]. For instance, in the context of induction motor drives, combining reference model selection with adaptive control methods has proven effective. By dynamically selecting appropriate reference models and adjusting control parameters in real time, these strategies maintain stability and performance, even in challenging environments with parameter fluctuations or external disturbances [1]. However, these methods often involve additional modeling and parameter optimization, which can be time-consuming. In multi-agent or swarm systems, such as fleets of drones, large numbers of similar systems are deployed simultaneously. Controllers are typically designed for specific operating conditions. While this fixed-design approach simplifies implementation and ensures reliability within predefined scenarios, it may struggle to adapt to system changes or unexpected events, such as hardware failures [3]. Applying adaptive control to each system individually could be computationally intensive, potentially requiring high-performance computing resources.

To address these limitations, the concept of model transfer and selection control has been proposed. This approach leverages shared models and pre-trained controllers to achieve rapid adaptation to varying states, conditions, or configurations with minimal computational overhead. By integrating model transfer mechanisms with dynamic model selection strategies, systems can swiftly identify and deploy the most suitable model, ensuring robust performance and fault tolerance [2], [3].

In this paper, we focus on theoretically understanding the performance of closed-loop control under changing and fault conditions and verifying the effectiveness of the model and controller sharing approach through practical case studies. Specifically, our main contributions are summarized as follows:

• We propose a shared model-based control framework that allows sharing of multiple models and controllers between systems of the same type and selecting the most suitable model and their controller based on changing and fault conditions. This approach not only facilitates rapid system adaptation to different operating conditions and fault scenarios, but also significantly reduces the computational overhead associated with real-time learning.

• Through extensive experimental validation using a real-world system, the Quanser Drone [4], we demonstrate how model transfer and selection methods effectively compensate for closed-loop system dynamics and significantly improve closed-loop system performance compared to systems without model transfer.

2. Methodology

In the proposed framework, for a large number of systems, we assume that a small proportion of the systems are modeled and have controllers designed for them. These models and controllers are used as repository. For the remaining or the newly introduced systems of the same types, the most appropriate models are selected from the existing repository without the need to construct new models or redesign controllers, thereby reducing computational cost and improving overall efficiency.

2.1. Multi-model transfer and selection frame

This section introduce the components of multiple model transfer and selection framework, detailing model construction, controller integration and switching, and model selection strategy.

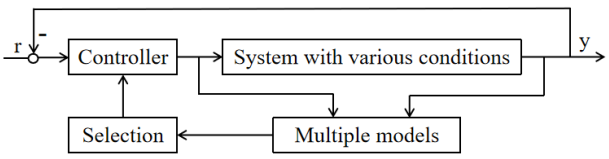

Fig. 1: Frame of multiple model transfer and selection

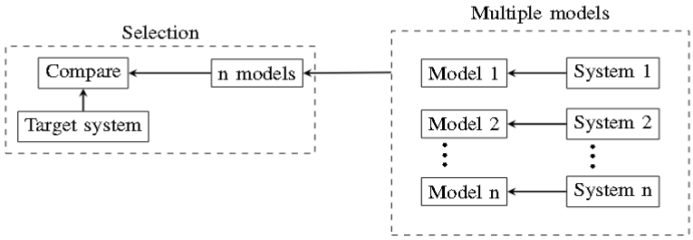

Fig. 2: Flowchart of multiple models and selection

The flowchart in Fig.1 depicts a closed-loop control system that combines dynamic model selection with feedback control to ensure adaptability and performance under varying conditions. The process begins with the reference signal (r), which represents the desired system state. The Controller receives the error signal, calculated as the difference between the reference signal (r) and the feedback signal (y) from the system's output. This closed-loop structure allows the system to self-correct by continuously monitoring. The multiple models from different systems stores a set of models, representing different system characteristics and operating conditions. Selection module evaluates the current system state, and match the appropriate model from multiple models module. After determining the suitable model, it is integrated into the controller, ensuring that the control actions align with the current system dynamics and operating condition.

The description in Fig.2 enables new systems to reuse the existing models stored in the multiple model set. The process consists of two main stages: multiple models collection and model selection. In the first stage, Model 1 to Model n constructed from System 1 to System n, forming a multi-model set. In the second stage, the target system's characteristics are compared with the multi-model set to evaluate its compatibility. If the target system matches one or more models, its controller can be shared with the target system. This approach is particularly suitable for handling a large number of systems of the same type that exhibit variations due to manufacturing differences. Through dynamic matching and integration, the framework ensures efficient control for systems with similar characteristics, while allowing for continuous expansion of the model library to accommodate unique systems when necessary.

Fig.3 shows the process of the adaptability evaluation of the new system under varying conditions based on the multiple model method. Different from the first approach, this frame emphasizes systems across a range of conditions, including both normal operation and faults. The multiple model set, a global collection, contains models for all systems (w systems) under these varying conditions. From this set, a specific working condition model is selected to represent either the operating characteristics of the target system, or the working conditions it shares with the target conditions.

2.2. Second-order Linear Dynamic Model

There are many types of linear and nonlinear dynamic models. In this study, the widely used dynamic model is adopted. Each system is associated with a corresponding model which effectively represents its dynamic characteristics.

The original open-loop system is described using a second-order linear dynamic model, which transfer function is given by Equation (1), where K represents the steady state gain (The ratio of the final steady-state value of the output to the

input value when the input is a unit step signal), ω_n denotes the natural frequency given by Equation (2). The oscillation period of the system, determined as $= \frac{t_n - t_1}{n-1}$, where t_1 is the time of the first peak in the first oscillation, t_n is the time of the *n-th* oscillation peak, and n is the total number of oscillation. Equation (3) represent the calculation of damping ration ζ, which quantifies the degree of attenuation in oscillations. The decrement ratio, defined as $\delta = \frac{1}{n} log(\frac{o_1}{o_n})$, where o_1 and o_n are the amplitudes of first and *n-th* oscillation,respectively. This approach offers a detailed quantitative analysis of the system's dynamic behavior. The pitch angle and rotor speed responses are used to calculate ω_n and ζ, which quantify the system's oscillatory behavior, including its frequency and decay rate. These parameters are then substituted into the transfer function to derive a complete linear second-order system model.

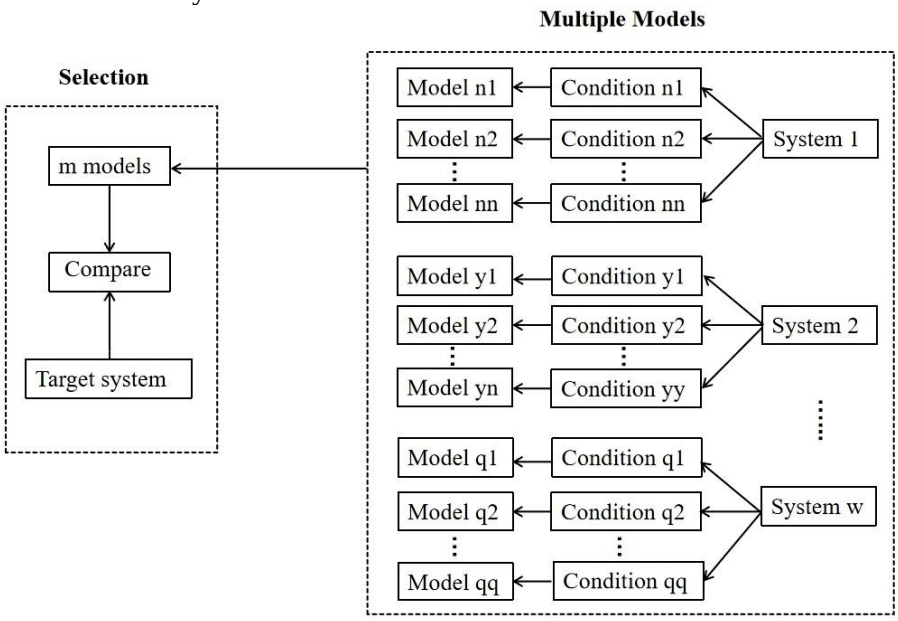

Fig. 3: Flowchart of multiple models and selection under varying conditions

$$G(s) = \frac{K\omega_n^2}{s^2 + 2\zeta\omega_n s + \omega_n^2} \tag{1}$$

$$\omega_n = \frac{2\pi}{T} \tag{2}$$

$$\zeta = \frac{1}{\sqrt{1 + (\frac{2\pi}{\delta})}} \tag{3}$$

2.3. Proportional Integral Derivative (PID) Controller

The controller is designed, tuned, and optimized based on the second-order model to ensure precise control and system stability. Controller selection should consider system characteristics, dynamic performance requirements, constraints, and computational resources. Due to its simplicity, robustness, and real-time efficiency, the Proportional-Integral-Derivative (PID) controller is widely used.

In this paper, a modified PID controller is utilized. For the derivative component, sharp changes in the reference signal, such as step changes, can produce a "kick" which is undesirable. To address this issue, a widely adopted modification is applied by excluding the derivative action on the reference signal as Equation (4). It can also be rewritten as Equation (5),

$$V(s) = K_p E(s) + \frac{K_i}{s} E(s) - K_d s\theta(s) \tag{4}$$

$$V(s) = K_p [E(s) + \frac{E(s)}{T_i s} - T_d s\theta(s)] \tag{5}$$

$$T_i = \frac{K_p}{K_i} \tag{6}$$

$$T_d = \frac{K_d}{K_p} \tag{7}$$

where the proportional gain (K_p), integral time constant (T_i), and derivative time constant (T_d) are defined. Instead of applying the derivative term to the error signal E(s), it is applied exclusively to the output signal, as illustrated in Fig.4.

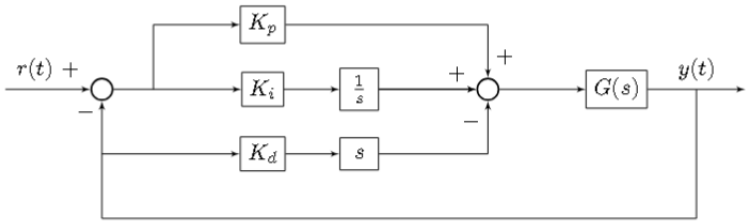

Fig. 4: Closed-loop with modified PID controller.

2.4. Method for Comparing Models

The two-step model selection process combines dynamic characteristic matching for preliminary screening with response-based evaluation for final selection. In the first step, the key dynamic characteristics, namely nature frequency (ω_n), damping ratio (δ), and system gain (k) are extracted from new system. These parameters are compared with the whole of candidate models parameters (ω_{nx} , δ, k_x, x approximately from 1 to 60) using the following error equation (6), where C_1, C_2, and C_3 are weighting coefficients that reflect the relative importance of ω_n , δ, and k of each candidate model respectively. The magnitude of system gain is significantly smaller than that of the other parameters, so its weight is appropriately increased to ensure it contributes adequately to the comprehensive error (C_1 =0.2, C_2 =0.2, C_3 =0.6). E_x represents the weighted comprehensive error for each candidate model, where x indicate the x^{th} Quanser Aero, labeled sequentially from 1 to m. Models with small E_x value are consider more similar to the new system. This step narrows down the set of candidate models about 10 models as subset.

$$E_x = C_1|\omega_n - \omega_{nx}| + C_2|\zeta - \zeta_x| + C_3|k - k_x| \tag{8}$$

After collecting the subset models, a more refined comparison is performed. In this stage, the output response of new system is compared with the subset models. By analyzing the closeness of these responses, the model that matches the new system is selected. This two-stage process ensures that the selected model closely aligns with the dynamic characteristics and behavior of the target system.

3. Experiments and Results

3.1. Method for Comparing Models

A real-word case study uses Quanser Aeros, which are numbered from No.1 to No.60. These are reconfigurable dual-rotor aerospace systems. Although they belong to the same type, the 60 systems exhibit differences due to manufacturing variations. As a result, 60 distinct second-order linear models are derived to establish the model set for subsequent model transfer and selection.

The Aero system has two rotors, each driven by a DC motor. It supports a 2-DOF (Degrees of Freedom) configuration, allowing control of both pitch and yaw angles. However, for this study, the yaw axis is locked, and the pitch angle is controlled by varying the speed of one of the DC motors. The swarm of Aeros provides an ideal platform for evaluating the model transfer and controller selection under varying and faulty conditions.

3.2. Model transfer from different systems of the same type

This section investigates the feasibility of model transfer and controller sharing among a group of Quanser Aero systems with inherent dynamic variations caused by manufacturing differences. The process is broadly divided into two steps: (1) constructing multiple models and their corresponding controller sets, and (2) selecting the most suitable model and controller through a systematic evaluation process. The dynamic responses of all 60 Aero systems are analyzed based on their rotor speed and pitch angle, with key features such as oscillation period and the peak amplitudes of the first and nth oscillations extracted. Using Equations (2) and (3), the natural frequency (ω_n), damping ratio (δ), and gain (k) are calculated for each system, resulting in 60 second-order linear models.

No.2 Aero is randomly selected as the target system, while the remaining systems are considered candidate systems. Based on Equation (8), weighted comprehensive errors (E_1 to E_{60}) between the target model and each candidate model are calculated, the top 10 systems with the smallest values are preliminary selected and recorded in Table 1. Controllers are also designed for each of these 10 systems with parameters K_p, T_i and T_d, which are also listed in the Table 1.

Table 1: Quanser Aero PID Controller Parameters

Aero No.x	ω_n	δ	k	E_x	K_p	T_i	T_d
2(target)	0.698	0.074	0.0045	0.000	730	2.50	1.0
14	0.804	0.076	0.0041	0.021	800	2.35	1.0
10	0.813	0.069	0.0045	0.023	960	2.11	1.4
5	0.852	0.012	0.0044	0.032	750	1.00	2.0
3	0.768	0.023	0.0055	0.036	1400	2.80	1.0
15	0.881	0.059	0.0047	0.039	1000	2.00	1.0
16	0.944	0.063	0.0044	0.046	800	2.50	1.0
20	0.953	0.090	0.0056	0.054	700	2.00	1.0
13	1.008	0.042	0.0034	0.066	950	2.20	1.3
4	1.072	0.044	0.0039	0.081	500	2.00	2.0
8	1.070	0.035	0.0032	0.083	700	1.70	2.0

To refine the selection process, four smallest $E_x$value of candidate models (E_{14}=0.021, E_{10}=0.023, E_5=0.032, E_3=0.036) are chosen for further evaluation. The model and controller No.14, No.10, No.3, and No.5 Aero are applied to the target system (No.2 Aero). The resulting system step responses are compared, and the model that produces the closest match to the target system is No.14, as illustrated in Fig.6. This observation suggest that the model from Aero No.2 and No.14 are likely similar. This demonstrates the ability of certain systems to share models and controllers. Subsequently, the controller designed for the target system is further transferred to other Aero systems to evaluate the transferability of the model and controller. The results are shown in Fig.7. At steady state, the output response curve of Quanser Aero No.50 closely matches that of the target system (No.2) and exhibits a smaller overshoot compared to the other candidate systems. While the output responses of systems No.7 and No.31 have rise times similar to that of the target system, both No.7 and No.31 exhibit larger steady-state errors and higher overshoots.

Based on the results shown in Fig.6 and Fig.7, both the No.14 and No.50 Quanser Aero exhibit output responses closely matching those of the No.2 Quanser Aero, in terms of transient behavior (rising time and overshoot). To further validate the cross transferability of the controllers, the No.14 controller was applied to the No.50 device, and the results are presented in Fig.8. The results demonstrates that the dynamic responses of No.14 and No.50 exhibit a high degree of similarity, as evidenced by the overlap of their response curves. This highlights the potential for efficient controller selection and transfer across different devices. These results demonstrate the feasibility of the proposed approach for model transfer and control, enabling robust performance across different systems of the same type.

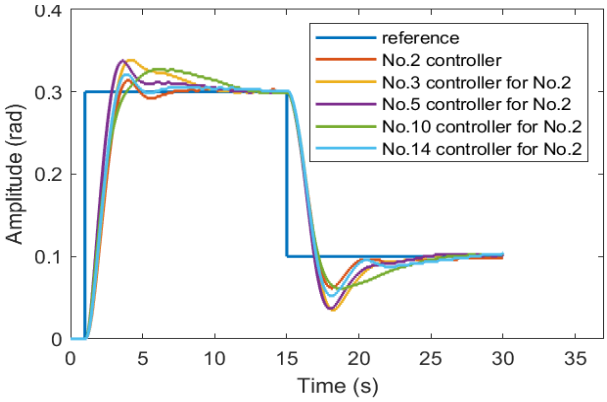

Fig. 6: Different controllers used on No.2 Aero.

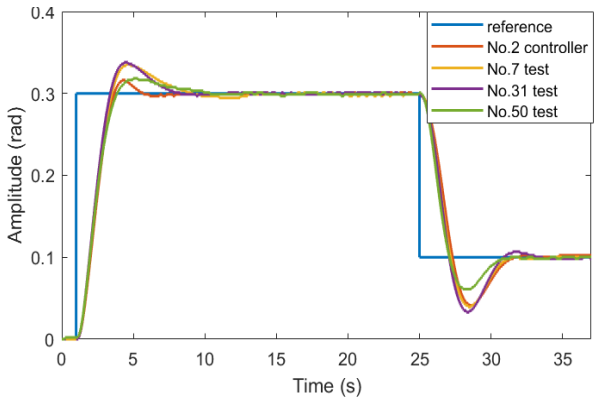

Fig.7: No.2 Aero controller used on others.

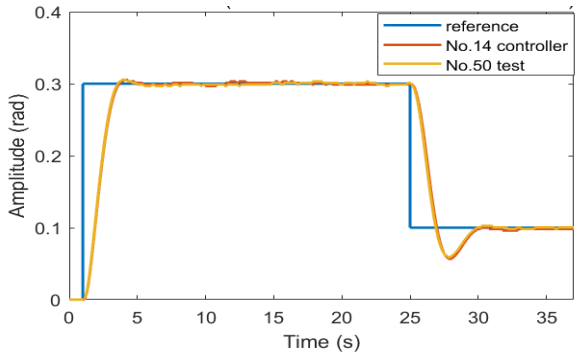

Fig. 8: No.50 Quanser Aero use No.14 controller.

Table 2 : Quanser Aero PID Controller Parameters.

Aero Number	Blade length	Selected Controller
No. 2	100% length	Controller A
No. 14	100% length	Controller A
No. 2	80% length	Controller B
No. 14	80% length	Controller B
No. 2	60% length	Controller C
No. 14	60% length	Controller C
No. 2	40% length	Controller D
No. 14	40% length	Controller D

3.2. Model transfer under damaging condition

This section focuses on model transfer and controller selection under damaging conditions, simulated by reducing blade length to create three distinct damage levels, along with the original undamaged blade, resulting in a total of four blade setups. Since the dynamic characteristics of Aero No.2, No.14, and No.50 have been previously verified as similar, the pre-designed models A, B, C, and D can be matched with any of these three systems when blade damage occurs, allowing the selection of the most suitable controller for the affected system.

The following presents the model selection process for handling blade damage on Aero No.2 and Aero No.14, demonstrating how the pre-designed models and controllers are matched to the damaged systems to ensure effective pitch angle control. To simulate blade damaging conditions, blades of varying lengths (100%, 80%, 60%, and 40% of the original length) were manufactured using 3D printing to represent the normal condition (100%) and three damage conditions (80%, 60%, and 40%), while maintaining the same material composition. The undamaged blades were printed in black, whereas the damaged blades were printed in white, as shown in Fig.9.

For each blade lengths (four different conditions), step response tests were conducted on the No.2 Aero to extract key system parameters, which were then used to derive four distinct second-order linear models. Correspondingly, PID controllers A, B, C, and D were designed to accommodate the dynamic variations introduced by each of four damaged cases, ensuring effective pitch angle control. The controller parameters (K_p, T_i and T_d) were fine-tuned based on performance criteria such as rise time and overshoot to achieve good control performance. To evaluate the transferability of the identified models and controllers, they were applied to the No.14 Aero under identical blade configurations. The results, presented in Fig.9, indicate that although the rise time observed in No.14 Aero is slightly longer compared to No.2 Aero, the system ultimately reaches a stable state and maintains effective pitch angle control. This further validates the dynamic similarity between the two Aero systems and demonstrates the feasibility of model and controller transfer.

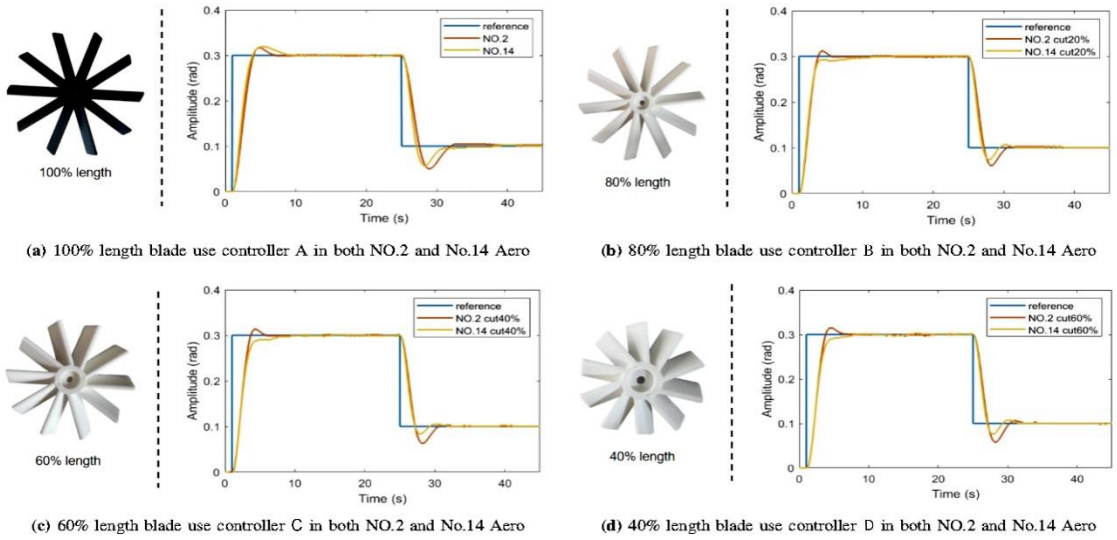

(a) 100% length blade use controller A in both NO.2 and No.14 Aero

(b) 80% length blade use controller B in both NO.2 and No.14 Aero

(c) 60% length blade use controller C in both NO.2 and No.14 Aero

(d) 40% length blade use controller D in both NO.2 and No.14 Aero

Fig. 9: Make controllers for different length blades.

Table 3 :100% Blade , Controllers, and Results.

Blades in Aero No.14	Controller	Overshoot (rad)	Rising time (s)
100%length	**A**	**0.02**	**5.52**
100%length	B	0.02	6.51
100%length	C	0.05	10.74
100%length	D	0.18	9.44

Table 4 : 80% Blade , Controllers, and Results.

Blades in Aero No.14	Controller	Overshoot (rad)	Rising time (s)
80%length	A	0.08	10.61
80%length	B	0.02	10.38
80%length	**C**	**0.00**	**9.57**
80%length	D	0.00	12.54

Table 5 :60% Blade , Controllers, and Results.

Blades in Aero No.14	Controller	Overshoot (rad)	Rising time (s)
60%length	A	0.03	10.21
60%length	B	0.00	10.24
60%length	**C**	**0.00**	**9.54**
60%length	D	0.00	12.23

Table 6 : 40% Blade , Controllers, and Results.

Blades in Aero No.14	Controller	Overshoot (rad)	Rising time (s)
40%length	A	0.01	15.53
40%length	B	0.00	13.31
40%length	C	0.00	13.98
40%length	**D**	**0.00**	**8.13**

Subsequently, tests were sequentially conducted on the Quanser Aero No. 14 device with blade lengths of 100%, 80%, 60%, and 40%, simulating various operating conditions. Based on the established models, the appropriate model and corresponding controller were matched for each condition through the processes of model transfer and selection. Fig. 10 shows the output responses of the four controllers (A, B, C, and D) applied under the condition of a 100% blade length. The control performance is also summarized in Table 3. Controller A produces the smallest overshoot and rise time values among the four controllers, indicating that Controller A, originally designed for the 100% blade, is effective in stabilizing the pitch angle of the full-length blade on the transferred device.

For a partially damaged blade (80% of its original length), all four controllers were tested, and the results are shown in Fig. 11. Controllers B and C outperformed Controllers A and D in terms of overshoot and rise time, with Controller C being slightly better than Controller B. This indicates that both Controller B, originally designed for 80% blade length, and Controller C, originally designed for 60% blade length, can be effectively transferred to Aero No. 14 with similarly damaged blades. For a more damaged blade (60% of its original length), the results are presented in Fig. 12 and Table 5. Controller C demonstrated the best performance in terms of overshoot and rise time, suggesting that Controller C, originally designed for the 60% blade length, can be effectively transferred to another system with a similarly damaged blade. In the case of a severely damaged blade (40% of its original length), results in Fig. 13 and Table 6 indicate that Controller D performed the best. This further confirms that Controller D, initially designed for the 40% blade, is also transferable to another device with a similar level of damage. These experimental results suggest that controller transfer remains effective under varying damage conditions.

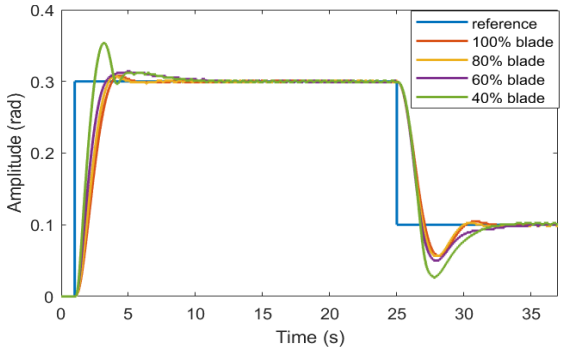

Fig. 10: Step responses under 100% length blades

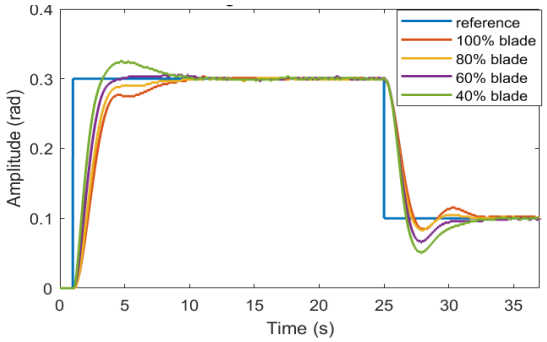

Fig. 11:Step responses with an 80% length blades

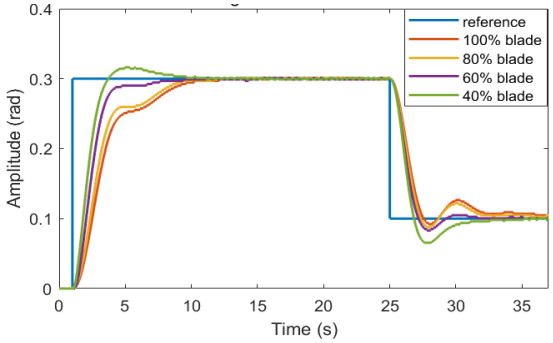

Fig. 12: Step responses under 60% length blades .

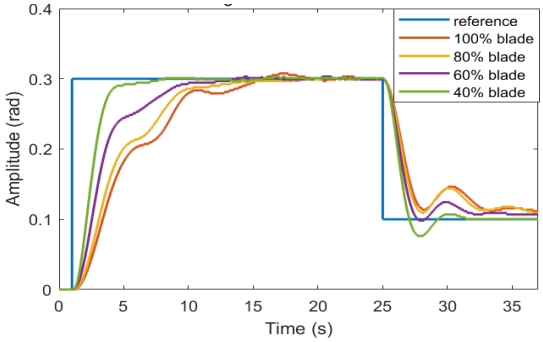

Fig. 13: Step responses under 40% length blades

4. Conclusion

This study presents a model transfer and selection control framework to enhance the adaptability and reliability of autonomous systems under varying and faulty conditions. By integrating multiple model sharing and selection strategies, the approach enables controller transfer between structurally similar systems and dynamic adaptation of control parameters. Validated through real-world experiments on the Quanser Aero platform, the framework is tested in two scenarios: model transfer between similar systems and model selection under structural damage. In both cases, pre-identified second-order linear models and PID controllers are successfully applied, ensuring stable pitch angle control while reducing manual tuning and computational costs. The results confirm the feasibility of multiple models transfer and controller sharing under varying conditions.

References

[1] K. J. ˚Astr¨om, “Adaptive control,” in Mathematical System Theory: TheInfluence of RE Kalman. Springer, 1995, pp. 437–450.

[2] R. Isermann, “Parameter adaptive control algorithms—a tutorial,” Auto- matica, vol. 18, no. 5, pp. 513–528, 1982

[3] Y. Naung, A. Schagin, H. L. Oo, K. Z. Ye, and Z. M. Khaing,“Implementation of data driven control system of dc motor by using system identification process,” in 2018 IEEE Conference of Russian Young Researchers in Electrical and Electronic Engineering (EIConRus), 2018, pp. 1801–1804

[4] Quanser, “Aero 2: Reconfigurable dual-rotor aerospace experiment for controls education and research,” 2022.